Journal of Magnetic Resonance **137,** 373–378 (1999)
Article ID jmre.1998.1689, available online at http://www.idealibrary.com on IDEAL®

A Tunable Reentrant Resonator with Transverse Orientation of Electric Field for *in Vivo* EPR Spectroscopy

Michael Chzhan, Periannan Kuppusamy, Alexandre Samouilov, Guanglong He, and Jay L. Zweier[1]

Molecular and Cellular Biophysics Laboratories, Department of Medicine, Division of Cardiology and the EPR Center, Johns Hopkins Medical Institutions, 5501 Hopkins Bayview Circle, Baltimore, Maryland 21224

Received July 29, 1998; revised December 15, 1998

There has been a need for development of microwave resonator designs optimized to provide high sensitivity and high stability for EPR spectroscopy and imaging measurements of *in vivo* systems. The design and construction of a novel reentrant resonator with transversely oriented electric field (TERR) and rectangular sample opening cross section for EPR spectroscopy and imaging of *in vivo* biological samples, such as the whole body of mice and rats, is described. This design with its transversely oriented capacitive element enables wide and simple setting of the center frequency by trimming the dimensions of the capacitive plate over the range 100–900 MHz with unloaded Q values of approximately 1100 at 750 MHz, while the mechanical adjustment mechanism allows smooth continuous frequency tuning in the range ±50 MHz. This orientation of the capacitive element limits the electric field based loss of resonator Q observed with large lossy samples, and it facilitates the use of capacitive coupling. Both microwave performance data and EPR measurements of aqueous samples demonstrate high sensitivity and stability of the design, which make it well suited for *in vivo* applications. © 1999 Academic Press

Key Words: in vivo **EPR spectroscopy; EPR imaging; reentrant resonator; transversely oriented electric field; free radical measurement.**

INTRODUCTION

With increasing interest in the role of free radicals in normal physiology and disease there has been a great need to develop instrumentation and techniques for *in vivo* measurement and imaging of free radicals. With recent advances in the development of instrumentation enabling EPR spectroscopy and imaging of *in vivo* biological samples these EPR techniques have become important tools for obtaining information regarding free radical metabolism in normal physiology and in the study of the pathophysiology of disease (*1–5*). Due to the special geometry and size of biological objects, development of specialized microwave components of the EPR instrumentation is of vital importance. The sample resonator and bridge must be tailored to the specific experiment and sample to provide optimized sensitivity and microwave field penetration. In our previous work, we have built L-band (1–2 GHz) instrumentation enabling high quality EPR spectroscopy and imaging of free radicals in biological samples of up to 25 mm in size (*6, 7*). We have performed high sensitivity spectroscopy and high quality spatial and spectral–spatial imaging of free radicals with submillimeter resolution in small *in vivo* or *ex vivo* systems (*8, 9*). However, there is a great need to measure and image free radicals in larger living systems so as to be able to answer fundamental questions regarding the role of free radicals, tissue oxygenation, and nitric oxide in the mechanisms of disease. Thus it is essential to develop high quality EPR resonator designs suitable for larger biological samples such as *in vivo* mice and rats (size up to 50 mm). It is also important to develop a sample resonator design that can be easily constructed and be readily adaptable for particular sample/frequency requirements, as well as provide high stability, sensitivity, and ease of operation.

We previously developed an approach for obtaining fixed-frequency EPR measurements of biological samples, utilizing a low phase noise fixed-frequency oscillator as a microwave source and an electronically and/or mechanically tunable ceramic reentrant L-band resonator, which is locked to the oscillator via a modified automatic frequency control (AFC) circuit (*10*). This approach is especially well suited for the low frequency EPR imaging of *in vivo* samples and has the following major advantages: the tunable resonator (1) enables the use of the extremely low phase noise fixed or narrow frequency tuning range oscillators, which offer improved spectral purity and stability; and (2) enables use of narrowband components in the bridge design, which provide better electrical characteristics.

The aim of the present manuscript is to describe the development and construction of a novel design of the two-loop one-gap reentrant ceramic resonator with transversely oriented electric field configuration, broad range mechanical resonant frequency tuning, and capacitive coupling. The resonator described was designed to work with a narrowband microwave bridge operating in the 750 MHz frequency range to enable *in*

[1] To whom correspondence should be addressed, at: Division of Cardiology, Johns Hopkins University School of Medicine, 5501 Hopkins Bayview Circle, Baltimore, MD 21224. Fax: 410-550-2448; e-mail: jzweier@welchlink.welch.jhu.edu.

1090-7807/99 $30.00

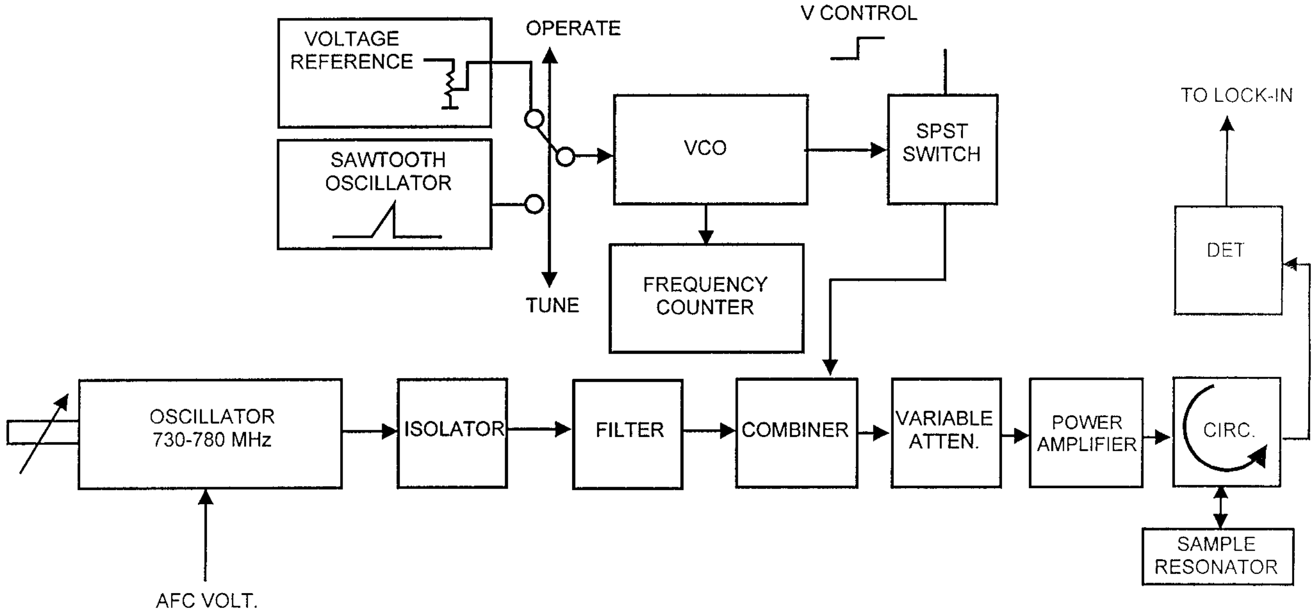

FIG. 1. Block diagram of RF bridge with a narrowband main oscillator and voltage-controlled oscillator for tuning visualization.

vivo EPR measurements of biological samples of up to 50 mm diameter, such as mice and small rats.

RESULTS AND DISCUSSION

A. Narrowband RF Bridge

A RF bridge utilizing a narrowband oscillator with electronic tuning for AFC modulation introduction was constructed at ~750 MHz (Fig. 1). The narrowband bridge approach makes it possible to take advantage of the improved performance of narrowband components such as lower phase noise of narrowband oscillators; lower losses of passive components; stable phase shift; better sensitivity and lower noise of a tuned detector; and, finally, availability of non-reciprocal devices for this frequency band (broadband ferrite circulators and isolators for frequencies under 1000 MHz are not practical due to prohibitive size and cost).

In this narrowband approach two problems must be addressed. First, a wider band sweep is needed to visualize the resonator mode. Second, variations in the resonant frequency of the resonator with samples of different size and loss parameters must be compensated. The first problem is overcome by a special provision for wider tuning sweep. As shown in Fig. 1, the bridge has two oscillators. The main low noise narrowband oscillator (Magnum Microwave, San Jose, CA) works in the "operate" mode, providing low noise bridge performance. In addition, an inexpensive Voltage Controlled Oscillator (VCO) (Minicircuits, Inc., Brooklyn, NY) with a wide tuning range substitutes for the main oscillator in the "tune" mode, allowing visualization of the resonator mode. A low noise amplifier (Cougar Components, Sunnyvale, CA) boosts the output signal of the main oscillator to up to 30 dBm. The second problem was addressed by introducing mechanical tuning of the resonant frequency of the sample resonator, as described below.

B. Reentrant Resonator with Transversely Oriented Electric Field (TERR)

The high stability/high *Q* ceramic reentrant resonators (RER), developed in our laboratory proved to be very efficient for *in vivo* EPR and imaging due to their dimensional stability and minimum thickness (*11*). These resonators were constructed to accommodate specific sample/frequency requirements. However, the geometry of this RER design makes it difficult to incorporate frequency tuning as well as capacitive coupling. The capacitive gaps in the RER structure are not easily accessible. In addition the three-loop two-gap design with circular reentrances, as used in our *L*-band and *S*-band resonators, becomes quite bulky and difficult to machine when scaled up for the 750 MHz frequency band.

Therefore a novel resonator design further optimized for large lossy biological samples at 750 MHz was constructed with mechanical resonance frequency tuning and provisions for electronic tuning and automatic coupling adjustments to be incorporated in future. As shown in Fig. 2, the structure contains two reentrant inductive loops of square cross section. The capacitive area of the resonator is formed by two plates protruding into the center of the resonator from the opposing sidewalls. The plane of the gap in the resulting flat capacitor is transverse to that in the conventional reentrant resonator. At the frequencies of interest (RF frequency band) this structure can be well approximated by a lumped circuit. The equivalent schematic of this type of resonator is shown in Fig. 3A along

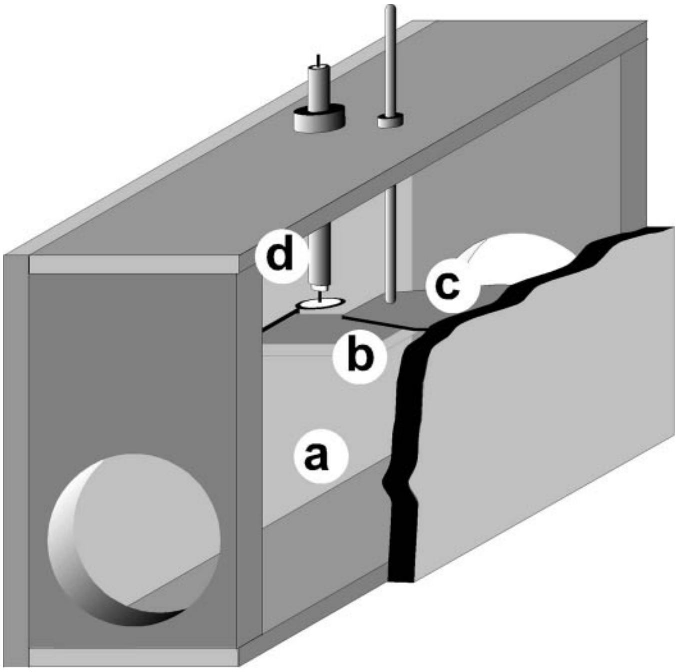

FIG. 2. Transversely oriented Electric Field Reentrant Resonator (TERR). (a) Inductive sample area. (b) Capacitive gap. (c) Flexible metal plate. (d) Coupling coaxial with a capacitive coupling plate.

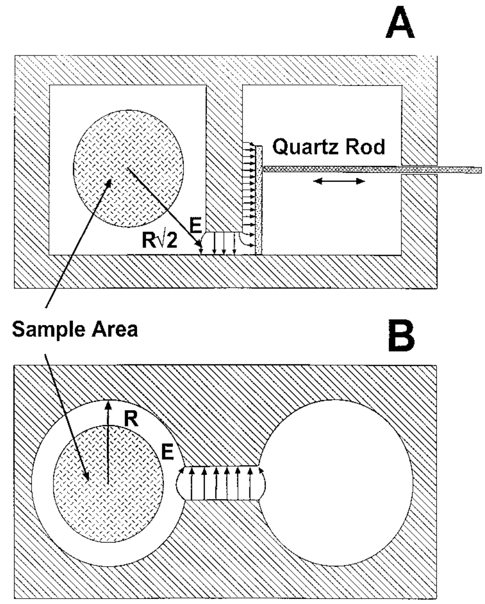

FIG. 4. (A) TERR cross section with lines of force of electric field *E* detail. The distance from the center of the sample reentrance to the area of fringe electric field is the square root of 2 greater than that for a RER (B) of the same sample reentrance diameter.

with a sketch of its cross section. The equivalent circuit and cross section of a two-loop one-gap RER of conventional design are shown in Fig. 3B for comparison. An in-depth theoretical analysis for calculation of center frequency and *Q*-factor of square cross-section reentrant resonators was previously reported (*12*). For the TERR design, at frequencies below 800 MHz based on that model, considering the structure as one turn toroidal inductance and lumped capacitor, a simple equation predicting the resonant frequency f_0 of the structure can be used,

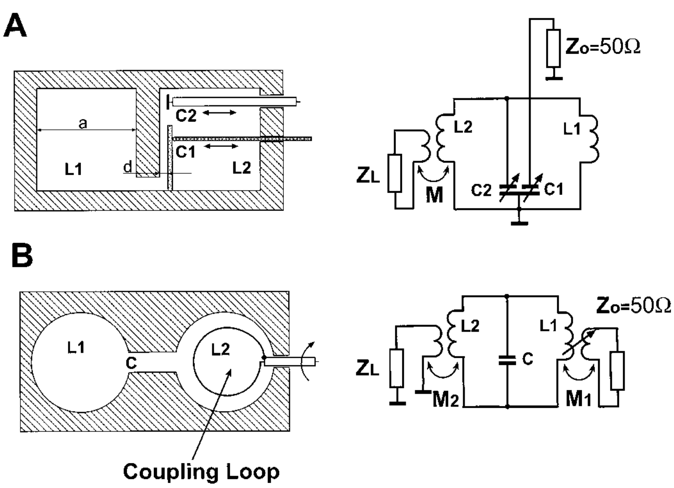

FIG. 3. (A) TERR schematic cross section and lumped circuit equivalent circuit. C1, resonance circuit capacitance; C2, coupling capacitance; L1, sample reentrance inductance; L2, coupling reentrance inductance; L2, coupling reentrance inductance; Zo, coaxial line impedance; ZL, sample impedance; M, magnetic coupling coefficient; a, width of square reentrance; d, capacitor gap thickness. (B) RER schematic cross section and lumped circuit equivalent circuit. C, resonant circuit capacitance; L1, sample reentrance inductance; L2, coupling reentrance inductance; Zo, coaxial line impedance; ZL, sample impedance; M1, M2, magnetic coupling coefficients.

$$f_0 = \frac{1}{2\pi a} \cdot \sqrt{\frac{ld}{\epsilon_0 \mu_0 s}},$$

where *a* is the width of the square reentrance; *d*, capacitor gap thickness; *s*, area of interleaving capacitor plates; *l*, length of the toroidal path along the center line of the resonator (see Fig. 3A). As shown in Fig. 4, the direction of the electric field lines in the capacitor formed by the plates of the proposed TERR is transverse to that in the conventional RER. Note that magnetic and electric lines of force in the TERR do not have to be orthogonal to each other due to the predominantly lumped circuit nature of the resonator. The distribution of the electric field component *E* is shown in Fig. 4. Panels A and B show the cross sections of the TERR and RER correspondingly with a circular sample of maximum radius *R* in the sample loop. As shown, the geometry of the TERR provides about square root of 2 greater distance from the center of the sample to the area of fringing electric fields. In addition, the fringing electric field is expected to be lower in the TERR since the electric field is mostly confined in the narrow gap between the stationary and movable plates. This concept is somewhat similar to that in the

TABLE 1
Specifications of the Prototype TERR

Parameter	Value
Overall dimensions outside (mm)	155 × 180 × 60
Dimensions inside (mm)	120 × 150 × 50
Center opening (mm)	50
Center frequency (MHz)	750
Center frequency (calculated) (MHz)	793
Center frequency setting range (MHz)	100–900
Center frequency tuning range (MHz)	±50
Unloaded Q without sample	1140
Unloaded Q with 30 g mouse	680
Maximum aqueous volume coupling capacity (ml)	100

recessed loop gap resonator design (*6*, *13*). Experimental quality factors Q of the resonator both without a sample and with a 30 g mouse are shown in Table 1.

Another important advantage of the TERR design is that the geometry of the resonator offers greatly improved accessibility to the capacitive region and, thus, enables convenient wide range frequency tuning by introduction of a flexible metal plate (c, Fig. 2) controlled by a precision linear movement mechanism. This is particularly important since tuning of the resonant frequency of the sample resonator is essential for practical implementation of the narrowband bridge approach, as noted above. This also allows incorporation of a simple wide range capacitive coupling mechanism (d, Fig. 2) into the structure. Capacitive coupling schemes widely used in NMR RF coils (*14*) are becoming more widely used in EPR instrumentation (*4*). In the inductive loop coupling scheme conventional for EPR the loop is generally not exactly orthogonal to the modulation field; the angular position of the loop depends upon the particular coupling needed. Thus the coupling loop may directly pick up the modulation signal. In that sense capacitive coupling is potentially superior to the inductive coupling which must be used with the standard RER, since it offers better decoupling from the field modulation which in turn minimizes field modulation induced dc offset of the signal. Capacitive coupling also eliminates the need for the large coupling loop, which is more prone to microphonic noise.

To achieve field modulation, coils were wound on the surface of a hollow thin wall tube fabricated from low loss cross-linked polystyrene material (Rexolite), which was inserted into the resonator coaxially with the sample. The coils had Golay configuration, measuring 80 mm in length and 40 mm in height, wound on 46 mm outer diameter tube surface, containing 20 turns each of 32 AWG copper enamel insulated wire, and connected in series. The turns were permanently attached to the surface of the tube with polystyrene low loss glue. The modulation depth of up to 3.5 G at 100 kHz was achieved with the Bruker modulation amplifier matched to the coils with a ceramic capacitor.

C. Construction and Fabrication Techniques

A photograph of the ceramic TERR is shown in Fig. 5. To achieve high mechanical stability and rigidity the resonator as well as temperature stability parts was constructed from an inexpensive and easily machinable alumino–silicate ceramic material from Cotronics Corporation (Brooklyn, NY). The fabrication process of the resonators using this material was described in detail earlier (*11*). All of the parts are rectangular blocks or plates and, thus, do not require intricate machining. After a high temperature cure, a conductive silver layer (Dupont 6216) was applied to the appropriate surfaces of the ceramic parts with a paintbrush and then fired in at 650°C. The parts of the resonator were assembled with Dupont 5504N silver-filled conductive epoxy and cured at 160°C. One of the side walls was attached permanently, while the other was attached with four screws with a silver foil gasket between conductive surfaces. This provided easy opening and adjustments to the resonator. The stationary capacitor plate was machined from ceramics and after silver plating was permanently attached to the wall with conductive epoxy. The movable capacitor plate was machined from 0.76 mm thickness beryllium copper plate, silver electroplated, introduced into the resonator through a slit in the opposite side wall, and permanently attached to it with Dupont 5504N conductive epoxy. By trimming the size of this plate the center frequency of the resonator can be initially set in a broad range. We were able to

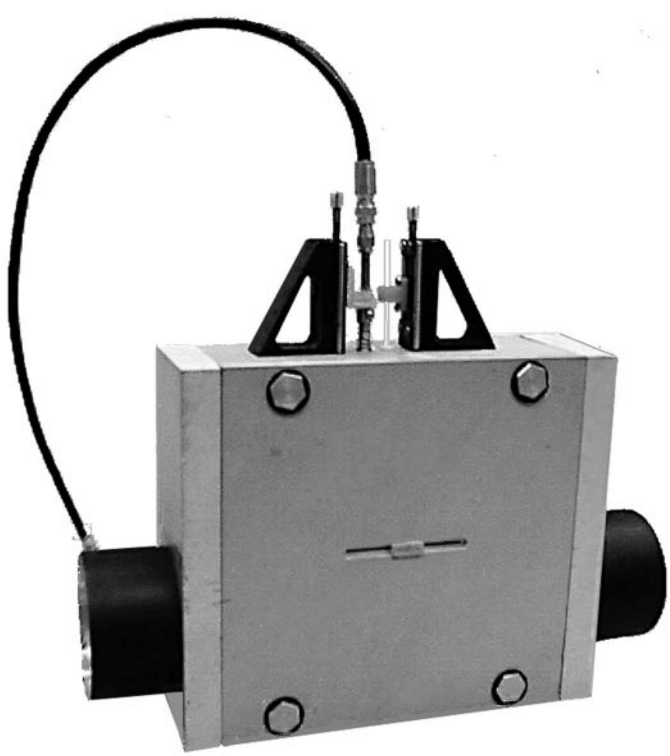

FIG. 5. Photograph of the ceramic TERR for 750 MHz with frequency tuning and capacitive coupling.

change the center frequency of the resonator from 100 to 900 MHz by adjusting the movable plate dimensions and its position in relation to the stationary plate. Two precision linear movement mechanisms were mounted on the side of the resonator (Edmund Scientific Company, Barrington, NJ). One of them is driving a 2 mm quartz rod pushing the movable capacitor plate. Changing the capacitance by moving this plate provides center frequency adjustment in the range ±50 MHz (about 13%). The mechanical adjustment of the center frequency was limited to this value to reduce microphonic sensitivity of the resonator. The second linear movement drives a rigid coaxial line with a 10 mm disk attached to the central conductor at the end of the line inside the resonator in the proximity of the stationary capacitor plate. This provides a wide capacitive coupling adjustment. The resonator can be critically coupled from its empty state up to 100 ml aqueous sample volume.

D. Test Results

The design and test data are summarized in Table 1. A high unloaded Q_0 of 1140 is achieved. An unloaded Q-factor of 680 is achieved with a 30 g mouse fully inserted into the center of the sample arm of the resonator.

The resonator was tested along with the narrowband 750 MHz RF bridge and Bruker 300-based spectrometer. The sensitivity was evaluated using an aqueous 30 ml sample of a 10 μM solution of the nitroxide spin label 2,2,6,6-tetramethyl-piperidine-1-oxyl, TEMPO, in a 25 mm diameter tube placed in the resonator. As shown in Fig. 6A, excellent sensitivity was observed with a signal to noise ratio of greater than 50 to 1. With *in vivo* measurements of nitroxides infused in living mice or rats high quality spectra were also observed. A spectrum of 1 cm^3 of 20 mM PCA injected into a 60 g rat (equivalent whole body concentration of approximately 400 μM) is shown in Fig. 6B. Some asymmetry of the spectrum was seen due to the non-uniformity of the modulation field along the length of the rat body. This can be overcome in principle by placing a larger set of modulation coils on the outside of the resonator in a magnet gap of sufficient size.

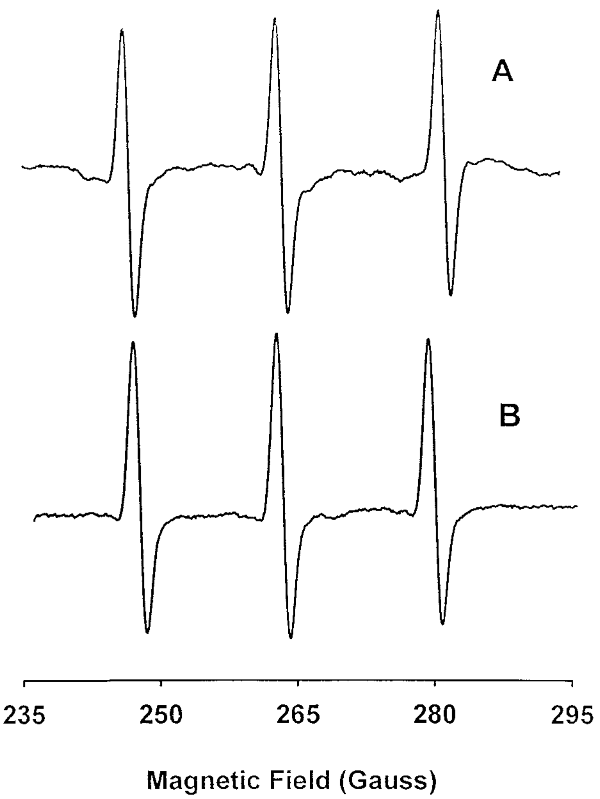

FIG. 6. (A) EPR spectrum of 30 ml of 10 μM 2,2,6,6-tetramethyl-piperidine-1-oxyl, TEMPO, in water obtained in the TERR resonator. Sweep width, 60 G; scan time, 60 s, time constant of the receiver 160 ms, number of scans 10, modulation frequency 100 kHz, modulation amplitude 0.5 G. (B) Spectrum of 3-carboxy-2,2,5,5-tetramethyl-1-pyrrolidinyloxy, PCA (1 cm^3, 20 mM solution in water) infused intravenously in a 60 g rat. Sweep width, 60 G; scan time, 60 s; receiver time constant, 320 ms; number of scans, 10; modulation frequency, 100 kHz; modulation amplitude, 1 G.

CONCLUSIONS

The TERR design described has a number of advantages over prior resonator designs. First, its transverse orientation of the capacitive gap provides easy access to the gap, which enables tuning of the resonator frequency. This enables the use of a narrowband microwave bridge with its intrinsically higher sensitivity. This design also facilitates the incorporation of capacitive coupling. Its transverse capacitive element limits electric field losses encountered with large *in vivo* samples, which potentially provides higher sensitivity for EPR measurements. It enables measurement of micromolar concentrations of free radicals in large lossy samples. The overall design flexibility allows for future modifications, such as introduction of electronic tuning for center frequency and coupling, which are important to further remove noise originating from the inherent instability of microwave losses of biological samples arising from motion, volume changes, or other sources. As such this design is well suited for EPR measurements and imaging of free radicals in living systems.

REFERENCES

1. G. R. Eaton, S. S. Eaton, and K. Ohno (Eds.), "EPR Imaging and *in Vivo* EPR," CRC Press, Boca Raton, FL (1991).
2. L. J. Berliner and H. Fuji, Magnetic resonance imaging of biological specimens, *Science* **227,** 517–519 (1985).
3. N. Kocherginsky and H. M. Swartz, "Nitroxide Spin Labels. Reactions in Biology and Chemistry," CRC Press, Boca Raton, FL (1995).
4. H. J. Halpern, D. P. Spencer, J. V. Polen, M. K. Bowman, A. C. Nelson, E. M. Dowey, and E. A. Teicher, Imaging radiofrequency electron spin resonance spectrometer with high resolution and

sensitivity for *in vivo* measurements, *Rev. Sci. Instrum.* **60,** 1040–1050 (1989).

5. R. K. Woods, J. W. Dobrucki, J. F. Glockner, P. D. Morse II, and H. M. Swartz, Spectral–spatial ESR imaging as a method of noninvasive biological oximetry, *J. Magn. Reson.* **85,** 50–59 (1989).
6. J. L. Zweier and P. Kuppusamy, Electron paramagnetic resonance measurements of free radicals in the intact beating heart: A technique for detection and characterization of free radicals in whole biological tissues, *Proc. Natl. Acad. Sci. U.S.A.* **85,** 5703–5707 (1988).
7. P. Kuppusamy, P. Wang, and J. L. Zweier, Three-dimensional spatial EPR imaging of the rat heart, *Magn. Reson. Med.* **34,** 99–105 (1995).
8. P. Kuppusamy, M. Chzhan, and J. L. Zweier, Development and optimization of three dimensional spatial EPR imaging for biological organs and tissues, *J. Magn. Reson. B* **106,** 122–130 (1995).
9. P. Kuppusamy, M. Chzhan, A. Samouilov, P. Wang, and J. L. Zweier, Mapping the spin density and lineshape distribution of free radicals using 4D spectral–spatial EPR imaging, *J. Magn. Reson. B* **107,** 116–125 (1995).
10. M. Chzhan, P. Kuppusamy, and J. L. Zweier, Development of an electronically tunable *L*-band resonator for EPR spectroscopy and imaging of biological samples, *J. Magn. Reson. B* **108,** 67–72 (1995).
11. M. Chzhan, M. Shteynbuk, P. Kuppusamy, and J. L. Zweier, An optimized *L*-Band ceramic resonator for EPR imaging of biological samples, *J. Magn. Reson. A* **105,** 49 (1993).
12. M. Giordano, F. Momo, and A. Sotgiu, On the design of a re-entrant square cavity as resonator for low-frequency ESR spectroscopy, *J. Phys. E: Sci. Instrum.* **16,** 774–779 (1983).
13. J. L. Zweier and P. Kuppusamy, *In vivo* EPR spectroscopy of free radicals in the heart, *Environ. Health Perspect.* **102,** 45–51 (1994).
14. J. Murphy-Boesch and A. P. Koretsky, An *in vivo* NMR probe circuit for improved sensitivity, *J. Magn. Reson.* **54,** 525 (1983).